Chemical Geology (Isotope Geoscience Section), 87 (1991) 175–196
Elsevier Science Publishers B.V., Amsterdam

Pb/Pb, Sm–Nd and Rb–Sr geochronology in the Archean Craton of Zimbabwe

P.N. Taylor[a,α], J.D. Kramers[b], S. Moorbath[a], J.F. Wilson[b], J.L. Orpen[b,β] and A. Martin[c]
[a]*Department of Earth Science, Oxford University, Parks Road, Oxford, OX1 3pR, United Kingdom*
[b]*Department of Geology, University of Zimbabwe, P.O. Box M.P. 167, Mount Pleasant, Harare, Zimbabwe*
[c]*8 Autumn Close, Harare, Zimbabwe*

(Received August 15, 1990; revised and accepted March 26, 1991)

ABSTRACT

Taylor, P.N., Kramers, J.D., Moorbath, S., Wilson, J.F., Orpen, J.L. and Martin, A., 1991. Pb/Pb, Sm–Nd and Rb–Sr geochronology in the Archean Craton of Zimbabwe. Chem. Geol. (Isot. Geosci. Sect.), 87: 175–196.

Pb isotope data for greenstone belt volcanic units, plutons and gneisses of the Archean Craton of Zimbabwe are presented together with Sm–Nd isotopic analyses and model Nd mantle derivation (t_{DM}) ages for selected samples. Pb/Pb whole-rock isochrons yield well-determined dates for the Cardiff Hill rhyolite of the Shamva-Harare greenstone belt (2659^{+38}_{-39} Ma), the Somabula tonalite (2752^{+50}_{-52} Ma), the Gwenoro Dam migmatitic gneisses (2705^{+60}_{-63} Ma), and for various suites from the Chingezi tonalite (from 2874 ± 32 to 2686^{+88}_{-94} Ma).

Comparison of geochronological results from this study with those of earlier work (mainly Rb–Sr whole-rock dating) shows some significant discordances, and their possible causes are discussed with regard to time-integrated Th/U ratios and the geological settings of the relevant rock units.

The Chingezi and Sesombi plutons show good agreement between Rb–Sr and Pb/Pb whole-rock isochron dates and also display a limited range of Th/U ratios, appropriate to a purely igneous differentiation history. Early to mid-Archean gneisses show large ranges of Th/U ratios, probably the results of U disturbances during metamorphism. In these rocks Pb/Pb dates may be older or younger than the corresponding Rb–Sr dates, but t_{DM} model ages generally agree with the older of the isochron results.

The behaviour of the Rb–Sr and U–Pb whole-rock systems during metamorphism may depend critically on the nature of the fluid phase evolved. CO_2-rich fluids appear to be implicated in U enrichment of early Archean gneisses at the Shabanie Mine. It is argued that CO_2-rich fluids may cause disturbance of the U–Pb system without resetting the Rb–Sr system, while a H_2O-rich fluid phase could have the reverse effect.

1. Introduction

The Archean Zimbabwe Craton is a classical granite–greenstone terrain (e.g., Wilson, 1979). Of volcanic and sedimentary sequences, which occur in typically synclinical greenstone belts, several generations can be recognized from field evidence. The granitic–gneissic portion of the terrain consists of tonalitic–granodioritic gneissic basement rocks which in one case clearly predate greenstone supracrustals (Bickle et al., 1975), and widespread granitoids which clearly postdate all these supracrustals and are therefore termed the late Archean granitoids. They comprise the (dominant) adamellitic Chilimanzi suite and the tonalitic Sesombi suite.

The time constraints on crustal evolution in the Craton have so far been provided mainly by Rb–Sr whole-rock isotopic studies (Hickman, 1974a, b, 1978; Hawkesworth et al., 1975,

Present addresses:
[α]Woodstock School, Mussoorie, Uttar Pradesh 248178, India.
[β]Geological Survey Department, P.O. Box 8039 Causeway, Harare, Zimbabwe.

0168-9622/91/$03.50

TABLE I

Comparison of ages from the literature (Rb–Sr ages recalculated for a Rb decay constant of $1.42 \cdot 10^{-11}$ a^{-1} where appropriate) and results from the present study

Geological unit	Method	Age ± 2σ error (Ma)	R_i	Apparent μ_1	Reference
Late Archean granitoids:					
Chilimanzi granite suite, combined	Rb–Sr	2,570±25	0.7040±0.0010		Hickman (1978)
Denda granodiorite + Rutope gneiss near Harare	Rb–Sr	2,680±104	~0.7030±0.0037		Baldock and Evans (1988)
Sesombi tonalite	Rb–Sr	2,633±140	0.7008±0.0008		Hawkesworth et al. (1975)
	Pb/Pb	$2,579^{+154}_{-173}$		7.8	this work
	Sm–Nd	2,680 (t_{DM})			this work
Somabula tonalite	Rb–Sr	2,594±80	0.7012±0.0004		Moorbath et al. (1977)
	Pb/Pb	$2,752^{+50}_{-52}$		8	this work
	Sm–Nd	2,740 (t_{DM})			this work
Greenstone belt supracrustals:					
Iron Mask Formation felsic volcanics	Rb–Sr	2,512±168	0.7038±0.0033		Baldock and Evans (1988)
	Sm–Nd	2,910 (t_{DM}) 2,742 (t_{CHUR})			Baldock and Evans (1988)
Cardiff Hill rhyolites	Pb/Pb	$2,659^{+38}_{-39}$		8.6	this work
	Sm–Nd	2,800 (t_{DM})			this work
Harare greenstone belt, Bulawayan metadacites	Sm–Nd	2,812, 2,853, 2,870 (t_{DM}) 2,616, 2,662, 2,717 (t_{CHUR})			Baldock and Evans (1988)
Harare greenstone belt, mafic and intermediate volcanics	Rb–Sr	2,670±60	0.7012±0.0001		Jahn and Condie (1976)
Bulawayo area felsic volcanics	Rb–Sr	2,615±28	0.7017±0.0008		Baldock and Evans (1988)
Kwekwe, mafic volcanics	Rb–Sr	2,480±140	0.7034±0.0006		Hawkesworth et al. (1975)
	Pb/Pb	$2,380^{+309}_{-394}$		8.8	this work
Kwekwe, Maliyami Formation	Rb–Sr	2,660±70	0.7010±0.0002		Hawkesworth et al. (1975)
	Pb/Pb	$2,867^{+171}_{-195}$		7.7	this work
Bulawayo, mafic volcanics	Rb–Sr	2,485±90	0.7015±2		Hawkesworth et al. (1975)
		$2,867^{+77}_{-81}$		7.9	this work
Kwekwe and Bulawayo areas, mafic volcanics (mixed suite from a number of greenstone belts)	Rb–Sr	2,690±90	0.7014±1		Jahn and Condie, (1976), also using data from Hawkesworth et al. (1975)
Belingwe greenstone belt, mafic volcanics	Rb–Sr	2,700±70	0.7029±2		
Suite of Kwekwe, Bulawayo and Masvingo greenstone belt, mafic volcanics (mixed suite from a number of greenstone belts)	Sm–Nd	2,640±140			Hamilton et al. (1977)
Upper Bulawayan, Belingwe greenstone belt	Pb/Pb (WR)	2,690±26			Chauvel et al. (1983)
Limestone, probably base of upper Bulawayan, Masvingo greenstone belt	Pb/Pb (WR)	2,839±33			Moorbath et al. (1987)

TABLE I (*continued*)

Geological unit	Method	Age ± 2σ error (Ma)	R_i	Apparent μ_1	Reference
Gneisses and granitoids of intermediate age:					
Gwenoro Dam gneiss	Rb-Sr	2,720 ± 60	0.7011 ± 0.0004		Hawkesworth et al. (1975)
	Pb/Pb	$2,705^{+60}_{-63}$		8.4	this work
Umwindsi gneiss near Harare	Rb-Sr	2,865 ± 135	0.7018 ± 0.0077		Baldock and Evans (1988)
Rhodesdale gneiss	Rb-Sr	2,700 ± 80	0.7015 ± 0.0004		Moorbath et al. (1977)
	Pb/Pb	$2,976^{+121}_{-132}$			Moorbath et al. (1977)
	Sm-Nd	2,990 (t_{DM})		8.5	this work
Chingezi gneiss	Rb-Sr	2,810 ± 70	0.7017 ± 0.0006		Hawkesworth et al. (1979)
Chingezi tonalite					
Locality *81/8*	Rb-Sr	2,818 ± 78	0.7016 ± 0.0002		this work
	Pb/Pb	$2,800^{+72}_{-76}$		8.2	this work
	Sm-Nd	3,050 (t_{DM})			this work
Locality *81/9*	Pb/Pb	2,874 ± 32		8.4	this work
	Sm-Nd	2,950 (t_{DM})			this work
Locality *81/10*	Rb-Sr	2,723 ± 102	0.7015 ± 0.0003		this work
	Pb/Pb	$2,825^{+94}_{-100}$		8.1	this work
Localities *81/14-17*	Rb-Sr	2,684 ± 102	0.7027 ± 0.0009		this work
	Pb/Pb	$2,686^{+88}_{-94}$		8.1	this work
	Sm-Nd	2,980 (t_{DM})			this work
All, except localities *9* and *14*A (18 samples)	Rb-Sr	2,772 ± 60	0.7015 ± 0.0003		this work
All combined (24 samples)	Pb/Pb Pb/Pb	2,925 ± 30		8.1	this work
Early Archean gneisses and granitoids:					
Tokwe gneiss	Rb-Sr	3,500 ± 400	0.701 ± 0.004		Hawkesworth et al. (1975)
10 samples	Pb/Pb	$3,215^{+300}_{-375}$		8.9	this work
6 samples	Pb/Pb	$3,475^{+87}_{-93}$		8.8	this work
	Sm-Nd	3,560, 3,600 (t_{DM})			Moorbath et al. (1986)
Shabani gneiss	Rb-Sr	3,495 ± 120	0.7000 ± 0.0010		Moorbath et al. (1977)
	Pb/Pb	$3,088^{+44}_{-46}$		9.0	this work
	Sm-Nd	3,460, 3,460, 3,240 (t_{DM})			Moorbath et al. (1986); this work
Mont d'Or granodiorite	Rb-Sr	3,350 ± 120	0.711 ± 0.002		Moorbath et al. (1976)
	Pb/Pb	3,345 ± 55		9.3	Taylor et al. (1984)
	Sm-Nd	3,640, 3,670 (t_{DM})			this work
Mushandike granodiorite	Rb-Sr	3,445 ± 260	0.7017 ± 0.0030		Hickman (1974a)
	Rb-Sr	2,917 ± 171			Moorbath et al. (1987)
	Pb/Pb	$2,946^{+125}_{-135}$		9.7	Moorbath et al. (1987)
	Sm-Nd	3,540 (t_{DM})			this work
Detrital zircons from Archean sediments in southern part of Zimbabwe Craton	U-Pb	abundance peaks at 3,200, 3,350, 3,460, 3,600 and 3800 Ma			Dodson et al. (1988)

WR = whole rock.

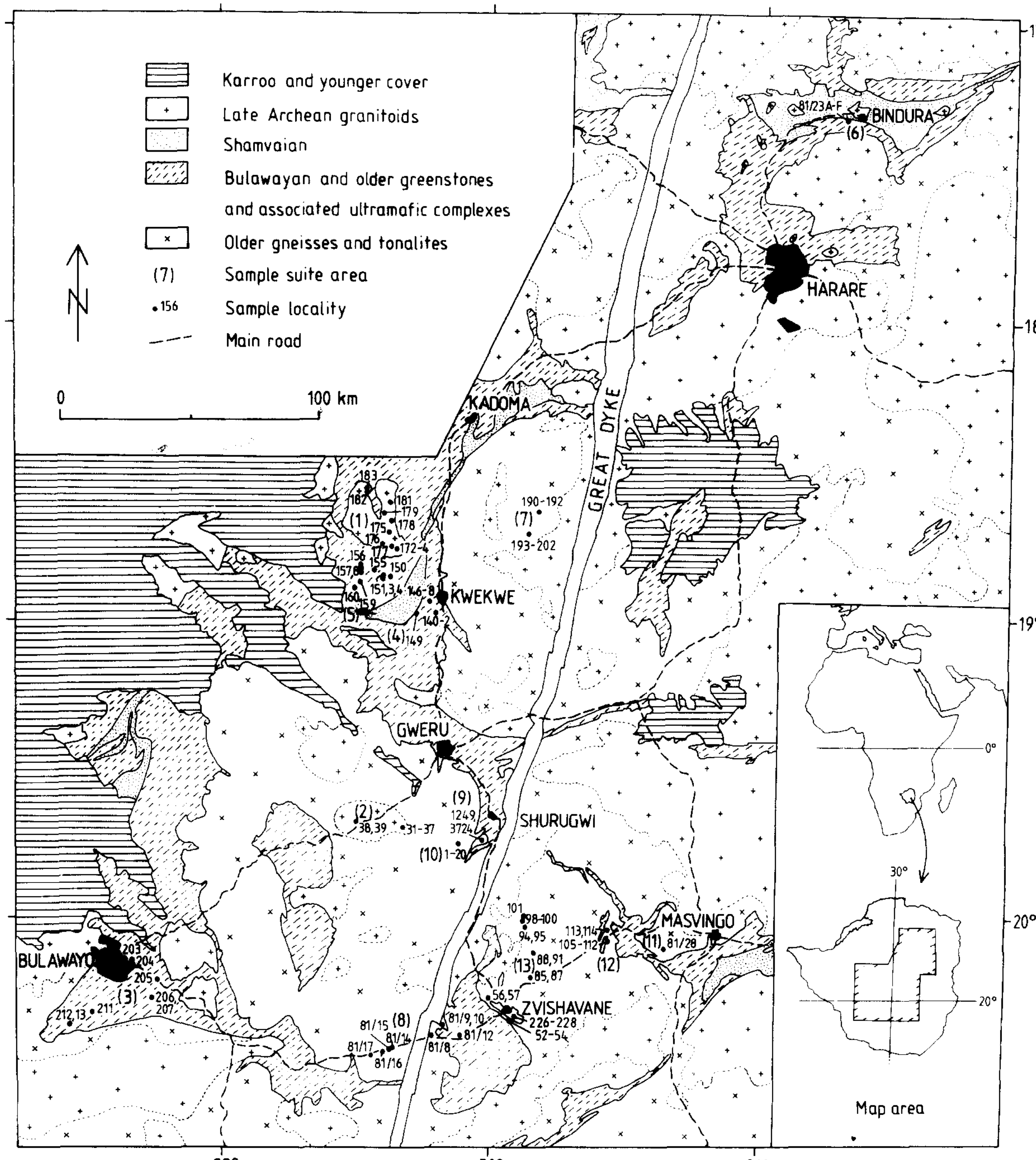

Fig. 1. Geological sketch map showing sample localities for the present study. All sample localities have prefix RH. Those shown with one *number* only have prefix RH*73/*. Suite localities are shown by *numbers in brackets*: *1*=Sesombi tonalite; *2*=Somabula tonalite; *3*=Bulawayo greenstone belt volcanics; *4*=Kwekwe greenstone belt volcanics; *5*=Maliyami Formation mafic volcanics; *6*=Cardiff Hill rhyolites; *7*=Rhodesdale batholith; *8*=Chingezi tonalite; *9*=Mont d'Or granodiorite; *10*=Gwenoro Dam gneisses; *11*=Mushandike granodiorite; *12*=Tokwe gneisses; *13*=Shabani gneisses.

1979; Jahn and Condie, 1976; Moorbath et al., 1976, 1977), complemented by Sm–Nd (Hamilton et al., 1977) and Pb/Pb work (Chauvel et al., 1983; Moorbath et al., 1987). The results have been largely summarized by Wilson (1979) and are compiled for reference in Table I. Two sets of results on greenstone belt volcanics (those of Jahn and Condie, 1976, and Hamilton et al., 1977) are from regionally collected suites comprising a number of greenstone belts. Most credibility has generally been attached to the whole-rock isochrons obtained on granitoids and gneisses. With the exception of a reconnaissance study on detrital zircons in Archean sediments (Dodson et al., 1988; Table I) which has shown the palaeoexistence of 3800-Ma-old rocks in the region, no zircon work on the Zimbabwe Craton has yet been published.

The studies have provided time-markers for the above-mentioned field geological subdivision, and established that the Zimbabwe Craton consists of (1) a relatively small triangular area between Shurugwi, Zvishavane and Masvingo (Fig. 1) of ~3.5-Ga-old gneiss terrain with infolded supracrustals of the "Sebakwian Group"— the "Mini-Craton" of Wilson (1979); (2) larger areas of 3.0–2.9-Ga granitoids, gneisses and volcanics (the latter defined as the Lower Bulawayan Group or Lower Greenstones); (3) extensive 2.7–2.6-Ga volcanic and sedimentary rocks (the Upper Bulawayan or Upper Greenstones); and (4) widespread 2.6-Ga plutons, ranging from tonalites to adamellites — the late Archean granitoids mentioned above. The emplacement of these was associated with cratonization. The end of the Archean crustal evolution in the Zimbabwe Craton is marked by the intrusion of the 2.5-Ga Great Dyke (Hamilton, 1977) along a fracture which cuts the craton from north to south.

In this paper we report further whole-rock Rb–Sr, Sm–Nd and Pb isotopic analyses of rock samples from the Zimbabwe Craton. Many of the samples included in earlier Rb–Sr studies have been analyzed for Pb, and some for Sm–Nd. In addition, some new sample suites have been analyzed. Sample localities are shown in Fig. 1. Our aim has been to confirm and refine the chronological constraints on crustal evolution in the Archean Craton of Zimbabwe, and further, to investigate the cause of the discordances which appeared between the results of the different dating methods.

2. Analytical methods

All samples were analyzed at the Department of Earth Sciences, Oxford University. Rb/Sr ratios were determined by X-ray fluorescence analysis on pressed powder pellets to better than ±1%. Sr samples for isotopic analysis were prepared using standard cation exchange, loaded on single Ta filaments and analyzed on a VG Isomass® *54*E fully automated mass spectrometer. $^{87}Sr/^{86}Sr$ ratios have been corrected for mass fractionation by normalizing to a value of 8.37521 for $^{88}Sr/^{86}Sr$. Analyses of the Eimer & Amend® standard on this instrument give results within error of ±0.70800, so no other correction has been applied to the Sr data reported in this work.

Pb samples for isotopic analysis were prepared by bomb dissolution followed by the Pb extraction using the double electrodeposition method of Arden and Gale (1974). Pb samples were loaded on single Re filaments with H_3PO_4 and silica gel. Most samples were analyzed on the 12-in. (~30.5 cm) radius 90° sector mass spectrometer designed and built at Oxford by N.H. Gale, but some were run on the VG Isomass® *54*E instrument. Measurements of NBS *981* and *982* Pb isotope standards on both mass spectrometers indicate mass fractionation factors between −0.14 and −0.10% a.m.u. through the course of this work. The results have been corrected accordingly. Pb blanks using the electrodeposition separation were generally ±10 ng during the course of this work. No correction was made for the blank since all ample preparations involved the separation of several μg of Pb.

Samples for Sm–Nd analyses were subjected to bomb dissolution. The rare-earth elements (REE) were separated as a group using cation-exchange columns, then Sm and Nd were separated on reverse phase chromatographic col-

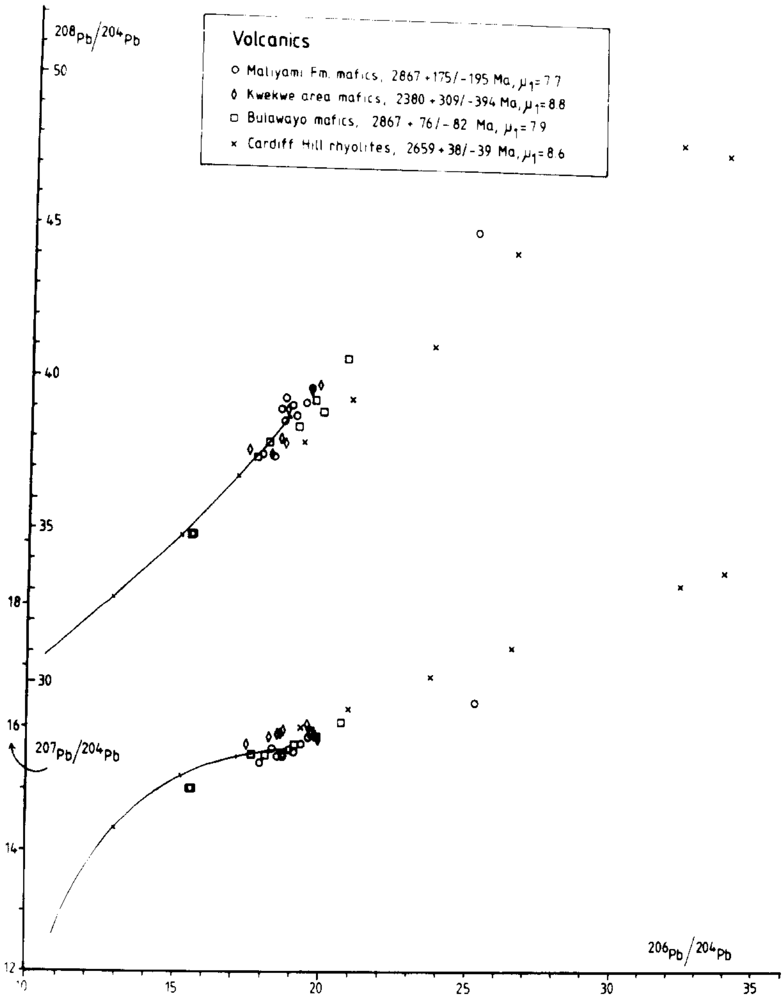

Fig. 2. $^{208}Pb/^{204}Pb$ and $^{207}Pb/^{204}Pb$ vs. $^{206}Pb/^{204}Pb$ plots of data from upper Bulawayan greenstone belt volcanics. All samples included in the regressions. Growth curves (Stacey and Kramers, 1975) drawn in purely for reference purposes.

umns with hydrogen di-ethylhexyl phosphate (HDEHP) supported on Teflon® powder, eluting with HCl. Sm and Nd concentrations were determined by isotope dilution using a mixed ^{149}Sm–^{150}Nd spike solution. Nd isotopic compositions were determined on the spiked Nd preparations. Sm and Nd samples for isotopic analysis were loaded on the Ta side filaments of a triple-filament assembly with a Re centre filament, and run on the VG Isomass® 54E instrument.

Pb isotopic analyses are reported in Table III, and Sm–Nd analyses are given in Table V. Isochron results reported in Table I were fitted using the method of York (1969), and t_{DM} model ages were calculated using the procedure of DePaolo (1981). For age calculations the values of the decay constants were as follows: for ^{87}Rb, $1.42 \cdot 10^{-11}$ a^{-1}; for ^{147}Sm, $6.54 \cdot 10^{-12}$ a^{-1}; for ^{238}U, $0.155125 \cdot 10^{-9}$ a^{-1}; for ^{235}U, $0.98485 \cdot 10^{-9}$ a^{-1}; for ^{232}Th, $0.049475 \cdot 10^{-9}$ a^{-1}.

Model μ_1-values ($^{238}U/^{204}Pb$ ratios) were calculated for a single-stage model with t_0 (age of the Earth) 4.57 Ga, and the primordial $^{206}Pb/^{204}Pb$ and $^{207}Pb/^{204}Pb$ ratios 9.307 and 10.294, respectively. They are for reference and comparison only, and this procedure does not imply strict adherence to a single-stage model or this particular value for t_0.

3. Volcanic rocks

Direct age constraints on supracrustal rocks have not been well established by the Rb–Sr whole-rock method. Errors on apparent ages are large, and dates obtained may actually be younger than ages of the late plutons intruded into the supracrustals (Table I). Thus from the early studies, the age of the Upper Bulawayan was best constrained by age data on these late plutons. However, Sm–Nd and Pb/Pb whole-rock isochrons have now improved the constraints on the age of the Upper Bulawayan supracrustals (Hamilton et al., 1977; Chauvel et al., 1983; Moorbath et al., 1987; Table I).

Fig. 2 shows the Pb isotope data for the volcanic rocks analyzed in this study, all of them from the Upper Bulawayan. The greenstone belt mafic volcanics have been described by Hawkesworth et al. (1975); the Cardiff Hill rhyolite samples are from a felsic intercalation in mafic volcanics of the Shamva–Harare greenstone belt, which are commonly correlated with the Upper Bulawayan (Fig. 1; Table II). This suite has yielded a Pb/Pb age of 2659^{+38}_{-39} Ma, agreeing well with several other age determinations on Upper Bulawayan suites. Mafic volcanics have been dated at 2640 ± 140 Ma by Sm–Nd (Hamilton et al., 1977) and at 2690 ± 26 Ma by the Pb/Pb method (Chauvel et al., 1983). Another felsic volcanic suite has yielded a Rb–Sr whole-rock isochron date of 2615 ± 28 Ma (Baldock and Evans, 1988; Table I).

The Sm–Nd t_{DM} model age of 2.80 Ga for the Cardiff Hill rhyolite (Table V) is slightly older than the Pb/Pb isochron age, but taken together with the high model μ_1-value of 8.6 this discrepancy may indicate some contribution by older crust in the petrogenesis of the rhyolite. The same conclusion can be drawn from t_{DM} ages of 2812, 2853 and 2870 Ma ob-

TABLE II

Samples not described previously

Sample	Comments	Zimbabwe grid reference
Chingezi tonalite:		
RH*81/8* A,B,C,D	leucocratic tonalite, old Bulawayo–Zvishavane road close to junction with new road, near Great Dyke contact	QH *897403*
RH*81/9* A,B,C,D,E	leucocratic tonalite, Mtshingwe River, ~3 km downstream from Great Dyke	QH *984429*
RH*81/10* A,B,C,D,E,F,G	leucocratic tonalite, Mtshingwe River, ~2 km downstream from Great Dyke	QH *967435*
RH*81/12* C,D,E	tonalite clasts in vent breccia within Hokonui Formation, Mtshingwe River	QH *997420*
RH*81/14* A,B	A: gneissic; B: massive leucocratic tonalite, road Zvishavane–Bulawayo, 149 km peg	QH *719358*
RH*81/15* A,B	Gneissic tonalite, same road, 150.5 km peg	QH *705355*
RH*81/16* A,B	foliated white biotite–tonalite, same road, 153.5 km peg	QH *697353*
RH*81/17* A,B	foliated fine-grained grey tonalite, same road, 159 km peg	QH *638334*
Cardiff Hill rhyolites:		
RH*81/23* A,B,C,D,E,F	light- to dark-grey highly siliceous massive felsic volcanics, apparently single flow; NNW side of Cardiff Hill, Trojan Mine, Bindura	UR *175870*

TABLE III

Lead isotope data

Sample No.	$^{206}Pb/^{204}Pb$	$^{207}Pb/^{204}Pb$	$^{208}Pb/^{204}Pb$
Bulawayo area greenstone volcanics:			
RH73/203	19.875	15.864	38.926
204	19.090	15.750	38.447
205	18.126	15.527	37.940
206	15.537	14.986	34.882
207	15.602	15.015	34.946
211*	17.726	15.568	37.447
212*	19.640	15.925	39.301
213*	20.668	16.118	40.663
Maliyami Formation:			
RH73/150	19.036	15.617	38.775
151	17.859	15.409	37.587
153*	18.897	15.692	39.123
154	25.188	16.901	44.948
155*	18.674	15.612	39.338
156	18.525	15.533	38.984
157	18.613	15.552	38.673
158	19.578	15.748	39.737
159*	19.278	15.797	39.179
160*	18.307	15.688	37.415
Kwekwe greenstone belt volcanics:			
RH73/140	18.717	15.993	38.976
141	19.504	16.070	39.683
142	17.455	15.760	37.659
146	18.550	15.910	38.075
147	18.218	15.887	37.523
148	18.616	15.924	37.893
149*	19.889	15.822	39.805
Cardiff Hill rhyolites:			
RH81/23A	32.322	18.407	48.110
23B	19.272	16.025	37.958
23C	20.915	16.342	39.320
23D	23.666	16.884	41.150
23E	33.826	18.658	47.899
23F	26.450	17.360	44.247
Somabula tonalite:			
RH73/31	18.122	15.570	40.019
32	17.780	15.518	40.189
33	19.340	15.794	37.286
34	14.744	14.931	38.856
36	16.475	15.275	35.966
37	16.337	15.232	36.613
38	14.627	14.891	34.609
39	14.899	14.955	34.404

TABLE III *(continued)*

Sample No.	$^{206}Pb/^{204}Pb$	$^{207}Pb/^{204}Pb$	$^{208}Pb/^{204}Pb$
Sesombi tonalite:			
RH73/172	17.778	15.428	36.588
173	18.438	15.532	37.268
174	17.428	15.356	36.829
175	17.453	15.350	36.512
176	17.255	15.341	36.235
177	17.261	15.355	37.179
RH73/178*	17.307	15.397	35.917
179	18.831	15.608	37.984
181	17.983	15.470	35.470
182*	16.945	15.241	35.784
183	18.437	15.548	36.778
Gwenoro Dam migmatitic gneisses:			
RH73/01	18.078	15.717	38.087
02'	25.964	17.471	36.211
03	16.974	15.521	35.286
04	15.090	15.130	37.147
05	17.461	15.611	37.081
07*	25.887	17.358	37.121
RH73/08	19.689	16.120	41.597
09	19.436	16.064	36.268
10	16.426	15.409	39.325
11*	31.603	18.843	55.265
12	16.418	15.447	38.228
13	20.439	16.198	37.524
RH73/14	15.400	15.258	36.407
15	21.772	16.405	36.438
16	26.737	17.310	37.366
17	15.905	15.359	36.804
19	14.525	15.062	35.103
20	21.209	16.281	38.425
Rhodesdale gneisses:			
RH73/190	14.825	15.067	35.009
191	14.587	14.999	35.666
192	15.051	15.119	35.326
193	14.657	15.041	34.578
194	15.048	15.104	38.535
195	15.178	15.141	38.108
196	14.970	15.109	37.391
RH73/197	16.031	15.339	41.300
198	15.831	15.293	39.054
199	14.481	15.008	35.942
200	15.205	15.135	33.842
201	15.286	15.113	38.999
202	14.766	15.057	35.647
Chingezi tonalite:			
RH81/8A	16.111	15.256	35.622
8B	20.104	16.045	38.032

TABLE III *(continued)*

Sample No.	$^{206}Pb/^{204}Pb$	$^{207}Pb/^{204}Pb$	$^{208}Pb/^{204}Pb$
Chingezi tonalite (cont.):			
*8*C	18.386	15.712	36.439
*8*D	16.688	15.381	34.980
9A(*1*)	33.747	18.951	53.809
9A(*2*)	33.720	18.951	53.369
9B	27.601	17.668	47.879
9C	25.929	17.360	47.042
9D	32.213	18.628	52.840
9E	32.376	18.694	52.542
*10*A	15.072	15.010	34.593
*10*B	16.112	15.217	34.509
*10*C	15.839	15.177	34.743
*10*D	17.035	15.417	35.455
*10*E	15.778	15.161	35.209
*10*F	17.707	15.535	35.705
*10*G	17.075	15.420	35.426
*12*C*	17.377	15.447	34.770
*12*D*	16.270	15.232	34.658
*12*E*	15.948	15.172	34.440
*14*A	17.756	15.552	38.322
*14*B	17.398	15.496	37.575
*15*A	16.311	15.291	37.952
*15*B	16.994	15.417	37.007
*16*A	19.418	15.863	36.025
*16*B	18.698	15.716	38.443
*17*A	16.672	15.335	37.418
*17*B	17.267	15.484	37.697
Tokwe River gneisses:			
RH*73/105*	15.164	15.002	41.154
106	15.091	15.024	40.120
*107*A	15.326	15.036	34.841
*107*B*	16.780	15.327	35.207
108	16.054	15.275	38.279
110	15.141	15.024	37.507
*111**	15.342	15.243	36.977
112	18.369	15.985	37.313
*113**	14.434	14.957	35.820
*114**	14.332	14.924	34.859
Shabani gneisses:			
RH*73/52*	21.236	16.716	38.495
53	26.712	18.086	44.757
54	25.378	17.620	49.182
56	20.150	16.384	47.474
57	17.786	16.020	44.501
85	30.841	18.731	53.023
*87*B	22.212	16.879	50.481
88	19.314	16.225	42.496
91	15.235	15.373	37.418
94	14.727	15.184	35.653

TABLE III *(continued)*

Sample No.	$^{206}Pb/^{204}Pb$	$^{207}Pb/^{204}Pb$	$^{208}Pb/^{204}Pb$
Shabani gneisses (cont.):			
95	15.094	15.222	49.796
98	14.790	15.163	44.879
99	14.392	15.066	39.332
100	15.049	15.244	51.308
101	14.633	15.146	44.978
*226*A	18.978	16.293	39.959
*226*B	21.302	16.925	45.573
*226*C	40.448	21.015	61.307
*226*D	24.525	17.489	50.110
*227**D	66.129	25.825	58.152
*228*A	36.218	20.485	48.756
*228*B	32.888	19.512	45.658
*228*D	33.927	19.817	46.528

2 standard errors: ±0.1%.
*Not included in preferred regressions.

TABLE IV

Rb–Sr data of Chingezi tonalite

Sample	$^{87}Rb/^{86}Sr$	$^{87}Sr/^{86}Sr$	$\pm 2\sigma$ error
RH*81/8*A	0.1296	0.70681	0.00011
*8*B	0.2312	0.71101	0.00009
*8*C	0.2469	0.71173	0.00013
*8*D	0.4185	0.71850	0.00010
*10*A	0.2666	0.71201	0.00009
*10*B	0.1475	0.70725	0.00011
*10*C	0.1536	0.70748	0.00013
*10*D	0.3950	0.71660	0.00007
*10*E	0.2553	0.71164	0.00009
*10*F	0.2851	0.71287	0.00011
*10*G	0.2938	0.71315	0.00010
*12*C	0.2779	0.71249	0.00014
*12*D	0.2362	0.71060	0.00014
*12*E	0.1939	0.70928	0.00014
*14*A*	0.6029	0.72705	0.00009
*14*B	0.9266	0.73796	0.00009
*15*A	0.8421	0.73466	0.00007
*15*B	0.8477	0.73577	0.00011
*16*A	0.4908	0.72168	0.00014
*16*B	0.4638	0.72061	0.00010
*17*A	0.5160	0.72221	0.00009
*17*B	0.5221	0.72251	0.00015

*Not included in preferred regressions.

TABLE V

Neodymium data and model ages

Sample	Sm (ppm)	Nd (ppm)	$^{147}Sm/^{144}Nd$	$^{143}Nd/^{144}Nd$	t_{DM} (Ga)
Cardiff Hill rhyolite:					
RH*81/23C*	3.689	19.375	0.1154	0.511239	2.80
Sesombi tonalite:					
RH*73/179*	1.392	8.019	0.1049	0.511134	2.68
Somabula tonalite:					
RH*73/34*	2.444	16.153	0.0915	0.510846	2.74
Rhodesdale gneiss:					
RH*73/199*	1.311	7.974	0.0994	0.510809	2.99
Chingezi tonalite:					
RH*81/8*A	1.195	7.846	0.0920	0.510620	3.05
RH81/9C	2.755	13.732	0.1213	0.511265	2.95
RH*81/16*A	1.813	7.525	0.1457	0.511725	2.98
Tokwe gneiss:					
RH*73/106**	2.746	17.225	0.0964	0.510298	3.60
RH*73/111**	1.765	10.710	0.0996	0.510407	3.56
Shabani gneiss:					
RH*73/53**	7.022	43.283	0.0981	0.510436	3.46
RH*73/226*A*	6.064	29.880	0.1227	0.511004	3.46
RH*73/227*D	4.938	26.115	0.1143	0.510945	3.24
Mont d'Or granite:					
RH*73/1249*	3.901	24.293	0.0971	0.510265	3.67
RH*73/3742*	3.785	25.260	0.0906	0.510132	3.64
Mushandike granite:					
RH*81/28*B	2.081	13.435	0.0936	0.510277	3.54

2σ error on $^{143}Nd/^{144}Nd$ ratios: 0.000020. Depleted mantle model of DePaolo (1981).
*Data from Moorbath et al. (1986), for comparison.

tained on Bulawayan dacitic volcanics from the Harare area by Baldock and Evans (1988; Table I, reported by the authors in the form of t_{CHUR} ages).

In other volcanic suites, Pb isotope data presented here give dates which are significantly older or younger than the well-defined and mutually consistent data on the Upper Bulawayan volcanics described above. The Kwekwe mafic volcanics have a high apparent μ_1-value of 8.8 corresponding to an implausibly young apparent age of 2380 Ma, albeit with very large uncertainties of $^{+309}_{-324}$ Ma. In two other units, the Maliyami Formation and the Bulawayo mafic volcanics, somewhat high apparent ages of 2867^{+171}_{-195} and 2867^{+77}_{-81} Ma, respectively, correspond to low apparent μ_1-values of 7.7 and 7.9, respectively. Implausible apparent ages are thus accompanied by improbable μ_1-values in a manner which suggests that the slopes of the arrays for these suites in the Pb/Pb diagram are not a function of age alone. As possible other factors, variable crustal contamination on eruption, a heterogeneous source region or post-emplacement alteration could be invoked. The latter alternative is not very likely in view of apparently undisturbed Th/U ratios (see p. 190).

4. Late Archean plutons

Two late Archean plutons studied, both belonging to the tonalitic Sesombi suite, are the Somabula and Sesombi tonalites (Fig. 1). The former was intruded into older gneisses, and the latter was emplaced into Upper Bulawayan greenstone belt rocks NW of Kwekwe (Fig. 1). Samples from the suites studied are described by Moorbath et al. (1977) and Hawkesworth et al. (1975), respectively.

The *Somabula tonalite* yields a well-defined Pb/Pb whole-rock isochron date of 2752^{+50}_{-52} Ma (Fig. 3), significantly older than

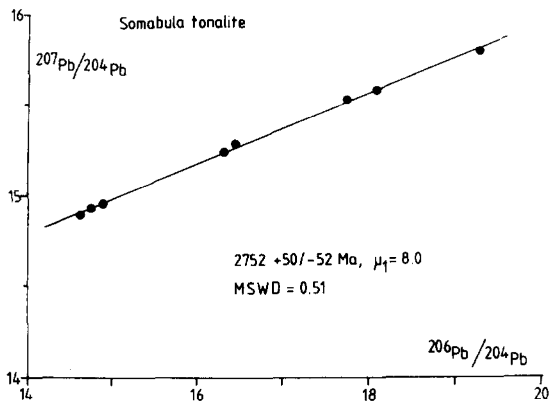

Fig. 3. $^{207}Pb/^{204}Pb$ vs. $^{206}Pb/^{204}Pb$ plot of data from the Somabula tonalite. All points included in the regression.

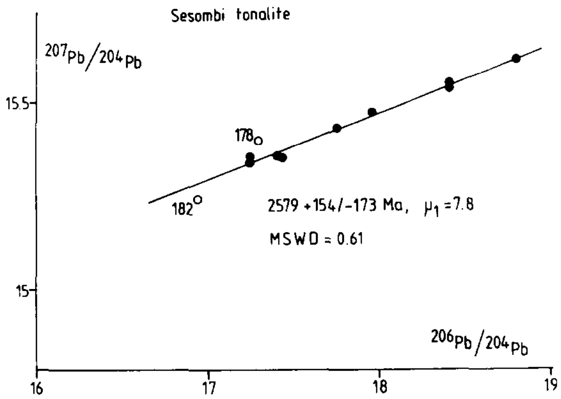

Fig. 4. $^{207}Pb/^{204}Pb$ vs. $^{206}Pb/^{204}Pb$ plot of data from the Sesombi tonalite. *Open symbols*: Not included in the regression.

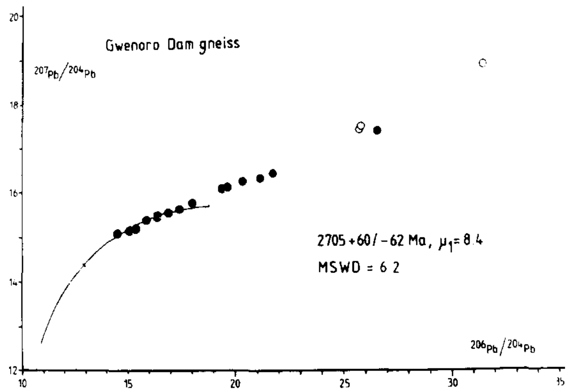

Fig. 5. $^{207}Pb/^{204}Pb$ vs. $^{206}Pb/^{204}Pb$ plot of data from the Gwenoro Dam migmatitic gneisses. *Open symbols*: Not included in the regression. Growth curve (as for Fig. 2) drawn in purely for reference.

the Rb–Sr age (2594 ± 80 Ma) but very close to the Nd model age of 2.74 Ga for this unit (see Tables I and IV). Thus the Pb/Pb isochron and Sm–Nd model age probably provide the best constraints on the age of this pluton, and the Rb–Sr isochron date is apparently too young.

The Pb/Pb isochron date for the *Sesombi tonalite* (2579^{+154}_{-173} Ma; Fig. 4) has a large uncertainty, which takes in both the Rb–Sr isochron result (2633 ± 140 Ma, Table I) and the t_{DM} model age (2.68 Ga, Table V). These results are therefore in mutual agreement, though not very precise.

Within the context of the Zimbabwe Craton, the Sesombi and Somabula plutons both have relatively low model μ_1-values of 7.8 and 8.0, respectively. Together with low initial $^{87}Sr/^{86}Sr$ ratios of 0.7008 ± 0.0008 and 0.7012 ± 0.0004, respectively, and concordant t_{DM} model ages, their model μ_1-values indicate that these plutons were new additions to the crust in the late Archean: No ancient crustal contributions to their parental magmas can be detected in their radiogenic isotope geochemistry.

5. Granitoids and gneisses of the mid- to late Archean

The *migmatitic gneisses at Gwenoro Dam*, 20 km southwest of Shurugwi (Fig. 1) were interpreted by Stowe (1968) as the oldest rocks in the area, and he tentatively regarded them as pre-Sebakwian. The gneisses are well exposed in the spillway of the dam, where banded gneisses with amphibolitic layers have been intruded, lit-par-lit, by granodiorite. Pb isotope data for fifteen samples, mainly granodiorites, define an errorchron with an age of 2705^{+60}_{-63} Ma ($\mu_1 = 8.4$; Fig. 5), in good agreement with the Rb–Sr isochron date of 2720 ± 60 Ma (Table I) from the same suite of samples. Three other samples have radiogenic Pb isotopic compositions and plot above the errorchron line (Fig. 5): these were excluded from the regression. One of these, RH*73/11*, a fine-grained mafic gneiss, plotted above the Rb–Sr isochron of Hawkesworth et al. (1975) and was also excluded from isochron fitting. Thus for most of the constituent rocks of the Gwenoro Dam gneiss complex the concordant results of Rb–Sr and Pb/Pb isochron dating can be accepted as providing a reliable age determination, but the presence of an older crustal component is suggested by the excess ^{207}Pb and radiogenic Sr in the excluded data points, and by the model μ_1-value of 8.4 for the other gneiss samples. This is rather high to represent pristine mantle-derived contributions to the crust at 2.7 Ga.

The large ovoidal area of gneisses and granites east of Kwekwe (Fig. 1) was termed the *Rhodesdale Batholith* by MacGregor (1951).

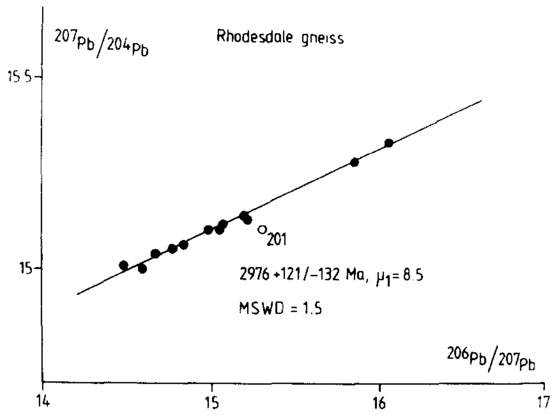

Fig. 6. $^{207}Pb/^{204}Pb$ vs. $^{206}Pb/^{204}Pb$ plot of data from tonalitic gneisses in the "Rhodesdale batholith". *Open symbol:* Not included in the regression.

The relationship between the Upper Bulawayan Midlands greenstone belt and the Rhodesdale gneiss has been obscured by shearing and the intrusion of ultramafic sills. However, the marked contrast in metamorphic grade between greenstone belt (very low grade) and gneiss (medium grade) strongly suggests that the Rhodesdale gneiss is basement to the Upper Bulawayan here (Robertson, 1976; Fabiani, 1989). Tonalitic gneiss samples from the central area of the batholith, and regarded by Stowe (1979) as the oldest unit, gave a 2700 ± 80 Ma Rb–Sr whole-rock isochron (Moorbath et al., 1977; see Table I) with an initial ratio of 0.7015 ± 0.0004. The Pb isotope data from the same samples yield a significantly older apparent age of 2976^{+121}_{-133} Ma, which is in good accord with the Sm–Nd t_{DM} model age of 2.99 Ga (Tables I and IV). Because of this good agreement between mantle derivation age and Pb/Pb errorchron age, the high model μ_1-value of 8.5 (Fig. 6) cannot indicate the presence of significant amounts of older crust, and was thus most likely inherited from a mantle source. The low initial Sr isotope ratio does not militate against the Rb–Sr age being reset, since the samples had very unradiogenic Sr themselves, indicating a crustal precursor with a low Rb/Sr ratio.

6. The early and mid-Archean plutons

The *Chingezi tonalite* intrudes the felsic volcanics of the Hokonui Formation, which underlie the basal unconformity of the Upper Bulawayan of the Belingwe greenstone belt (Martin, 1978). Yet a vent breccia within the volcanic sequence contains blocks of a lithologically very similar tonalite. The Chingezi tonalite may thus be coeval with at least part of the volcanic sequence and may represent its plutonic equivalent, with the roof of the pluton at a very high crustal level during emplacement. A foliated tonalitic unit to the south of the Chingezi tonalite has been designated as the Chingezi gneiss and dated by the Rb–Sr whole-rock method at 2810 ± 70 Ma, with an initial ratio of 0.7017 ± 0.0006 (Hawkesworth et al., 1979; Table I).

Chingezi tonalite samples for this study cover a fairly large area (Fig. 1; Table II). Samples include some slightly foliated varieties from west of the Great Dyke. The three samples from locality *81/12* are from tonalite blocks in the vent breccia within the Lower Bulawayan Hokonui Formation (see above). Geochronological results are summarized in Table I, and Figs. 7a–d and 8a–c. For the easterly suite RH*81/8* and the most westerly suite RH*81/14–17* the Pb/Pb whole-rock isochron dates of 2800^{+72}_{-76} Ma and 2686^{+88}_{-94} Ma agree well with the Rb–Sr dates of 2818 ± 78 and 2684 ± 102 Ma, respectively. For locality RH*81/10* the error limits between the Pb/Pb age of 2827^{+95}_{-101} Ma and the Rb–Sr date of 2723 ± 102-Ma overlap. The oldest Pb/Pb age (2874 ± 32 Ma) was obtained on the easterly suite RH*81/9*, which yielded no Rb–Sr date. The model μ_1-values vary between 8.1 and 8.4 (Table I; Rb–Sr data in Table IV). Interestingly, younger apparent ages are encountered in the more westerly suites, which are furthest away from the ~3.5-Ga mini-craton of Wilson (1979). The results for the easterly suites are also in accord with the 2810 ± 70-Ma Rb–Sr isochron date for the Chingezi gneiss (Haw-

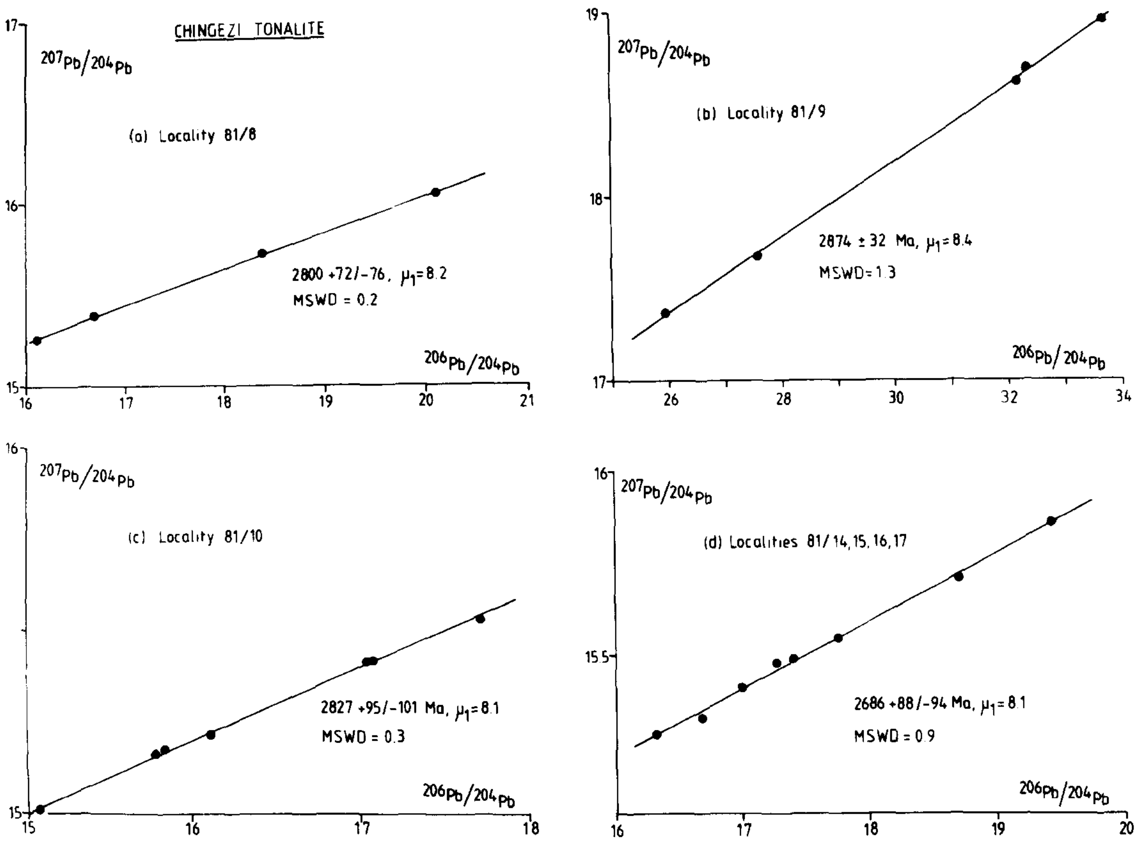

Fig. 7. $^{207}Pb/^{204}Pb$ vs. $^{206}Pb/^{204}Pb$ plots of data from individual sampling localities within the Chingezi tonalite, as indicated. All samples included in the regressions.

kesworth et al., 1979). However, t_{DM} model ages for three Chingezi tonalite samples (3.05, 2.95 and 2.98 Ga; Table I) are significantly older.

In view of the different dates and model μ_1-values obtained at the individual localities, the validity of a regional regression of all Chingezi tonalite Pb data is clearly questionable. Notwithstanding the comment, such a regression would yield a Pb/Pb date of 2925 ± 30 Ma (not shown) and, of all the Chingezi tonalite results discussed, this would give the closest agreement with the t_{DM} model age data. The three samples from the vent breccia (locality *81-12*) also plot on this regression. An equally questionable regression of the Rb–Sr data from all the sampling localities would yield a significantly younger "isochron date" of 2772 ± 60 Ma (Table I; not shown). In this case, the age discrepancy between the Pb/Pb and Rb–Sr dates merely illustrates the risk inherent in regional regressions, since the Pb/Pb and Rb–Sr results for individual outcrop suites are in agreement.

Variations in age and model μ_1 between localities appear to indicate that the Chingezi tonalite is composed of a series of intrusive bodies emplaced over a substantial interval of time, and derived from sources with differing U/Pb ratios. While the petrographic and Pb isotopic contrast between the samples from adjacent localities RH*81/9* and RH*81/10* lends support to this view, the uniform t_{DM} ages around 3 Ga show the existence of a common crustal parent body of this age, and the younger ages of the individual suites indicate crustal reworking, whether magmatic or hydrothermal.

The *Mushandike "granite"* is a dominantly

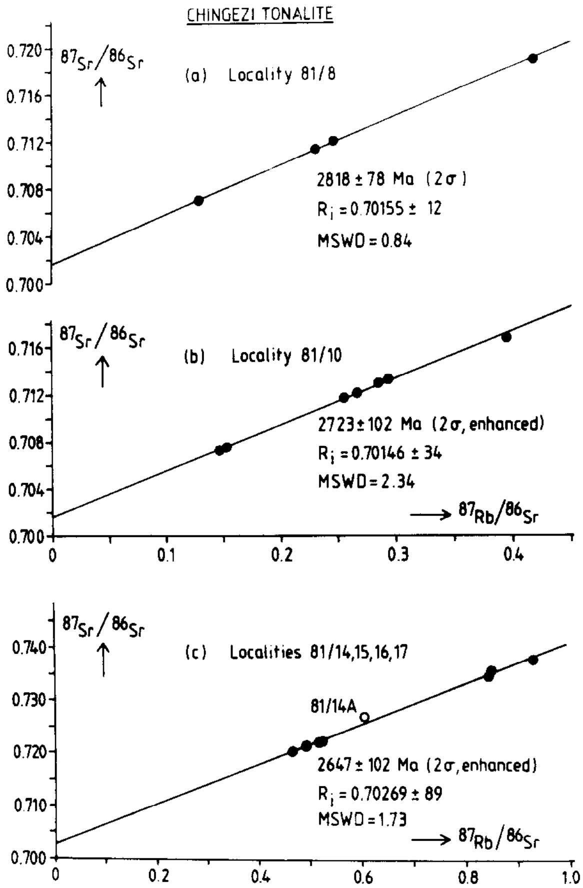

Fig. 8. $^{87}Sr/^{86}Sr$ vs. $^{87}Rb/^{86}Sr$ isochron plots of data from individual sampling localities within the Chingezi tonalite, as indicated. *Open symbol*: not included in the regression.

granodioritic pluton intrusive into surrounding gneisses west of Masvingo (Fig. 1). The first attempt to date the body, by the Rb–Sr whole-rock method, gave a 6-point 3445±260-Ma errorchron, with an initial Sr ratio of 0.7017±0.0030 (Hickman, 1974a). Subsequent Rb–Sr and Pb/Pb whole-rock studies have given dates of 2917±171 and 2946^{+125}_{-135} Ma, respectively, with an initial $^{87}Sr/^{86}Sr$ ratio of 0.710±0.002 and a model μ_1-value of 9.7 (Moorbath et al., 1987; Table I). The high initial Sr isotope ratio and apparent μ_1-value clearly indicate that remobilization of considerably older crust was involved in the ~2.9-Ga plutonic event, and the t_{DM} model age of 3.54 Ga reported in this work confirms that inference.

The *Mont d'Or "granite"* is actually a tonalitic–granodioritic intrusion into structurally complex ultramafic and supracrustal rocks of the Selukwe greenstone belt (Fig. 1). Previous age determinations by the Rb–Sr whole-rock method (Moorbath et al., 1976) and by Pb/Pb (Taylor et al., 1984) gave dates of 3350±120 and 3345±55 Ma, respectively, showing good agreement. The high $^{87}Sr/^{86}Sr$ initial ratio of 0.711±0.002 and model μ_1-value of 9.3 provide strong evidence that this pluton, old as it is, is derived by reworking of still more ancient continental crust. The t_{DM} model ages of 3.64 and 3.67 Ga for Mont d'Or samples reported in Table V reinforce that conclusion.

7. The early Archean gneisses

Very heterogeneous banded migmatitic gneisses crop out along the Tokwe and Shashe rivers near Mashava, between Masvingo and Zvishavane (Fig. 1). They contain infolded N–S-striking amphibolite-facies lenses of ultramafic and supracrustal rocks of the Sebakwian Group (Wilson, 1968). The *Tokwe River gneisses* have given a Rb–Sr whole-rock errorchron age of 3500±400 Ma (Hawkesworth et al., 1975; Table I). Sm–Nd model ages of 3.56 and 3.60 Ga (Table V) are in accord with this Rb–Sr date. The gneisses are migmatitic and show considerable strain. Syn- to post-deformational pegmatitic lenses and veins occur and are at least in part locally derived. In the light of this field evidence, the scatter of the Rb–Sr data is easily understood. The Pb isotope data show even more scatter (Fig. 9). The best-fit line for all Tokwe River gneiss samples has an MSWD-value of 124. It gives an apparent age of 3215^{+300}_{-375} Ma. A date of 3475^{+87}_{-93} Ma, together with a major improvement in quality of fit (MSWD=4), is obtained by omitting four of the ten data points — two of them from an

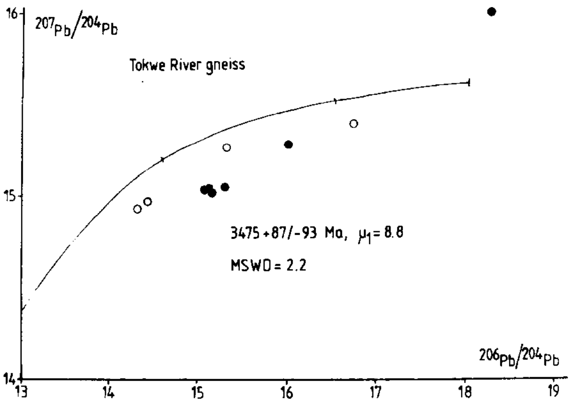

Fig. 9. $^{207}Pb/^{204}Pb$ vs. $^{206}Pb/^{204}Pb$ plot of data from the Tokwe River gneisses. *Open symbols*: not included in the regression. Growth curve (as for Fig. 2) drawn in purely for reference.

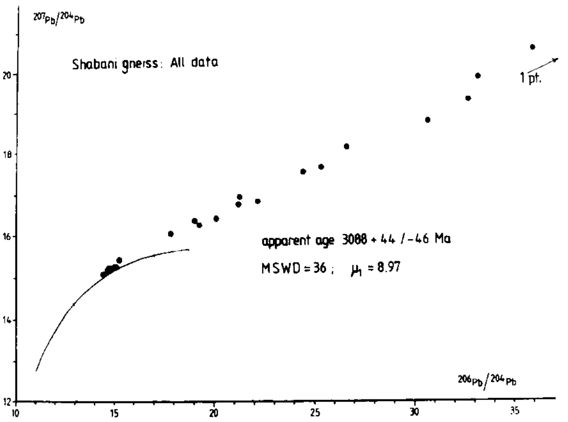

Fig. 10. $^{207}Pb/^{204}Pb$ vs. $^{206}Pb/^{204}Pb$ plot of data from the Shabani gneisses. All samples shown included in the regression; only most radiogenic sample (plotting off graph) rejected. This plots above regression line. Growth curve (as for Fig. 2) drawn in purely for reference.

outcrop at some distance from the main sampling sites. However, no petrographic features distinguish the rejected samples from the rest (Hawkesworth et al., 1975).

The *Shabani gneisses* constitute the eastern basement to the Upper Bulawayan of the Belingwe greenstone belt, the basal unit of which unconformably overlies the gneisses (Bickle et al., 1975). The Shabani gneiss samples have been taken from several outcrops covering a large area in the general vicinity of Zvishavane (formerly Shabani), as well as from the footwall of the Shabanie Mine. Rb–Sr whole-rock isochron dating has given a date of 3495 ± 120 Ma (Moorbath et al., 1977; Table I). This result is supported by two of the three Sm–Nd t_{DM} model ages obtained on Shabani gneiss samples (3.46, 3.46 and 3.24 Ga; Tables I and IV). Thus the Rb–Sr result is considered as a reliable determination of the age of formation of these gneisses. However, the Pb isotope data give a significantly younger apparent age of 3088^{+44}_{-46} Ma (Fig. 10). The Shabani gneisses show an enormous range of Pb isotope compositions, and a high apparent model μ_1-value of 9.0.

8. Discussion

From the preceding description of the results, and from Table I, observations about differences in ages obtained by the different methods can be summarized as follows:

(1) For the volcanic suites some large differences exist between Rb–Sr and Pb/Pb ages. Except in the case of the Bulawayo mafic volcanics, the large error limits of the Pb/Pb ages are such that no real significance can be attached to these differences.

(2) In most of the plutons considered in this study, Rb–Sr and Pb/Pb methods generally yield results in good agreement. In some cases the isochron dates are corroborated by Sm–Nd t_{DM} ages, but the Mont d'Or and Mushandike plutons have t_{DM} ages significantly greater than the isochron results, and also high initial $^{87}Sr/^{86}Sr$ ratios and apparent μ_1-values. The petrogenesis of these two plutons clearly involved reworking of older crust. The Somabula tonalite has Pb/Pb and Sm–Nd dates that are in good agreement, but a younger Rb–Sr isochron date.

(3) For the Rhodesdale and Shabani gneisses, the differences between Rb–Sr and Pb/Pb isochron dates are significant. These differences present the principal problematic discordances discussed in this paper.

In the Rhodesdale gneiss the Pb/Pb age of 2976^{+121}_{-132} Ma is older than the Rb–Sr age of 2700 ± 80 Ma, whereas the Shabani gneisses have a Rb–Sr whole-rock age of 3495 ± 120 Ma, older than the apparent age of 3088^{+44}_{-46} Ma given by the Pb/Pb method. In each case the t_{DM} age corresponds to the older of the age results obtained from Rb–Sr and Pb/Pb regressions. Thus it would appear that both Rb–Sr and Pb/Pb whole-rock systems may record Archean crust formation ages reliably, or may be disturbed or reset by later events.

Anatectic reworking of ancient crust results in differences between t_{DM} ages and the Rb–Sr and Pb/Pb isochron ages, as seen in the case of the Mushandike and Mont d'Or plutons. However, this process cannot easily account for the patterns of age discordance observed in the Rhodesdale and Shabani gneiss suites. To explain these, it is necessary to invoke processes in which the U–Pb system is disturbed while the Rb–Sr system remains intact, and vice versa. Such processes should also account for the development of the observed *apparent* isochrons or errorchrons. Recent or subrecent element mobilization can be excluded from consideration: It would generate scatter in the Rb–Sr isochron diagram, and have no effect on a Pb/Pb array.

The possible amount of early disturbance of the U–Pb system may be assessed by consideration of time-integrated Th/U ratios, determined from plots of $^{208}Pb/^{204}Pb$ vs. $^{206}Pb/^{204}Pb$ (Figs. 2 and 11). Th and U fractionation in magmatic processes is generally coherent, so that average terrestrial Th/U ratios, between 3.5 and 4, are maintained. Decoupling of the two elements might result from scavenging of U by fractionating minor phases, particularly zircon, or from oxidation of U to the hexavalent state in the presence of a mobile fluid phase. For the samples studied no evidence of U removal in zircon has been found by testing for appropriate chemical correlations (B. Lucas, pers. commun., 1991). Thus the high (up to 22) and low (down to 0.8) time-integrated Th/U ratios encountered in this study can probably be interpreted as reflecting U depletion or enrichment, respectively, by a fluid phase, with Th remaining immobile.

Variable losses or gains of U at any time between rock formation and the present generally cause scatter in the $^{207}Pb/^{204}Pb$ vs. $^{206}Pb/^{204}Pb$ diagram. However, reasonably good linear arrays could result under any of the following circumstances:

(1) U loss or addition is proportional to the original U content (considered highly unlikely).

(2) Variation in U/Pb ratios *after* U mobility greatly exceeds that originally present in the rock (Fig. 12).

(3) U loss is complete or almost complete (the classical secondary isochron).

(4) U loss or gain occurs either closely following rock formation or very close to the present.

The effects of U gains and losses on the slope of a regression line (and thence on the apparent age) are not always straightforwardly predictable, but in some cases U depletion can result in apparent ages older than the actual age of rock formation (Taylor, 1975; Griffin et al., 1978; Moorbath and Taylor, 1981, 1985; Welke and Nicolaysen, 1981; Moorbath et al., 1986). On the other hand, U gain may give rise to apparent ages intermediate between the rock formation and the U addition event.

For the mafic volcanic suites, the $^{208}Pb/^{204}Pb$ vs. $^{206}Pb/^{204}Pb$ plot (Fig. 2) indicates rather uniform time-integrated U/Th ratios in the range 3.2–4.2. Thus, although the greenstone belts were affected by an almost ubiquitous very low-grade to low-grade metamorphism in the late Archean, which was associated with much fluid migration, it appears that no major mobilization of U took place in the sampled units during this episode. As discussed above, the Pb/Pb dates for these suites are wrong and mostly have poor precision. This can now not be ascribed to U mobility, and initial Pb isotopic heterogeneity or Pb

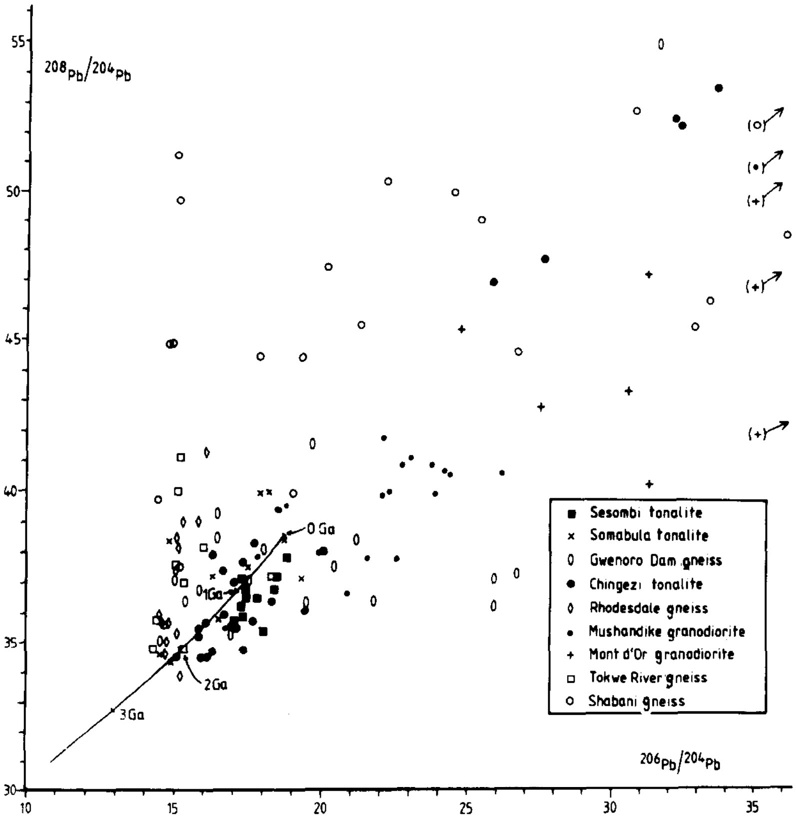

Fig. 11. $^{208}Pb/^{204}Pb$ vs. $^{206}Pb/^{204}Pb$ plot of all data from plutonic and gneissic suites obtained in this study, and from the literature (Mushandike: Moorbath et al., 1987; Mont d'Or: Taylor et al., 1984). Growth curves (as for Fig. 2) drawn in purely for reference.

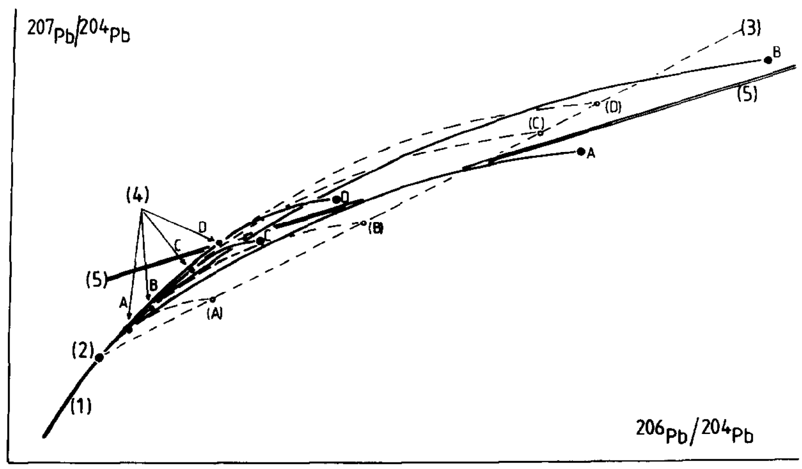

Fig. 12. Sketch $^{207}Pb/^{204}Pb$ vs. $^{206}Pb/^{204}Pb$ diagram to illustrate the clockwise rotation of a data array as surmised for the Shabani gneiss samples. *A–D* = hypothetical samples; *1* = "primary" Pb development; *2* = rock formation; *3* = Pb-Pb isochron that would have resulted without U remobilization, with *plotting* position for samples *in brackets*; *4* = synchronous but variable U remobilization; *5* = (*double line*) = resulting errorchron, giving approximate age of U remobilization only if the resulting spread in U/Pb ratios is large compared to original spread, and giving high apparent μ_1-value.

mobility remain as possible causes. The Cardiff Hill rhyolite suite shows slightly low time-integrated Th/U ratios around 2.8.

Of the plutons (Fig. 11), the Sesombi and Chingezi tonalites, and the Mushandike (Moorbath et al., 1987) and Mont d'Or (Taylor et al., 1984) granodiorites show similar small ranges of time-integrated Th/U ratios, between 1.5 and 4.5 (calculated using the apparent intrusion ages). These Th/U ratios are interpreted as plausible original (igneous) values, and it is suggested that these plutons have not suffered any post-intrusive disturbance to their U–Th–Pb systems. They also show good agreement between the Rb–Sr and Pb/Pb whole-rock isochron ages.

The Somabula tonalite has somewhat higher and more varied time-integrated Th/U ratios (see Fig. 11) with values from 2.5 to 17, though mostly <5.8. In spite of the discrepancy between its Pb/Pb date of 2752^{+50}_{-52} Ma and its Rb–Sr date of 2594 ± 80 Ma, the concordance of the former with a Sm–Nd t_{DM} model age of 2.74 Ga, and the good quality of fit of the Pb/Pb isochron (MSWD = 0.6) could be taken as evidence that the disturbances to the U–Th–Pb system implied by the Th/U variations were confined to a short time interval immediately following consolidation.

The four gneiss suites considered in this study all display scatter in time-integrated Th/U ratios (Fig. 11). The Shabani, Tokwe and Rhodesdale suites are generally characterized by high Th/U ratios (Shabani: range 1.8–22, average 7.3; Tokwe River and Rhodesdale: range 2–10; average 6). The Gwenoro Dam suite includes some very low Th/U ratios (range 0.8–8.8, average 4.1). Ages assumed for Th/U ratio determinations were 3.5 Ga for the Tokwe and Shabani gneisses, 3 Ga for the Rhodesdale gneiss, and 2.7 Ga for the Gwenoro Dam gneiss.

Rhodesdale and Gwenoro Dam both gave well-defined linear arrays in the $^{207}Pb/^{204}Pb$ vs. $^{206}Pb/^{204}Pb$ diagrams (Figs. 5 and 6). For Rhodesdale, the Pb/Pb isochron date of 2976^{+121}_{-132} Ma is concordant with the Sm–Nd t_{DM} model age of 2.99 Ga. These dates together provide the best constraint on the age of rock formation. Possible U losses implied by high Th/U ratios are thus most likely to have occurred during or immediately after rock formation. The Rb–Sr whole-rock age of 2700 ± 80 Ma is younger than the Sm–Nd and Pb/Pb age constraints, and this discrepancy is considered further below. For the Gwenoro Dam gneisses, Rb–Sr and Pb/Pb isochron dates are concordant at ~ 2.7 Ga, and this suggests that the very low Th/U ratios of some samples might have resulted from U addition, similarly close to the time of rock formation.

Pb isotope data for the Tokwe River gneisses are problematical: in the $^{207}Pb/^{204}Pb$ vs. $^{206}Pb/^{204}Pb$ diagram only six of the ten analyzed samples plot on a reasonable linear array (Fig. 9). The large scatter of data in the $^{208}Pb/^{204}Pb$ vs. $^{206}Pb/^{204}Pb$ diagram (Fig. 11) and the aberrant data points in the $^{207}Pb/^{204}Pb$ vs. $^{206}Pb/^{204}Pb$ diagram both suggest U mobility in at least some of the samples, significantly later than the formation of this gneiss complex.

The Shabani gneisses show concordance between the whole-rock Rb–Sr age of 3495 ± 120 Ma and two of the three Sm–Nd t_{DM} model ages (both 3.46 Ga). The Pb/Pb date of 3088^{+44}_{-46} Ma for the same rocks probably indicates disturbance of their U–Pb systems markedly later than the formation of the gneisses, as in the Tokwe River suite. The reasonably well-defined linear array in the $^{207}Pb/^{204}Pb$ vs. $^{206}Pb/^{204}Pb$ diagram (Fig. 10) is probably a consequence of U mobility having greatly increased the range of U/Pb ratios at the time of the disturbance [see case (2) on p.190 on linear arrays, and Fig. 12]. The high apparent μ_1-value of 9.0 for this suite requires that the stage of Pb isotopic evolution between formation of the gneisses and U mobilization took place with high U/Pb ratios. Those rocks with low present $^{206}Pb/^{204}Pb$ then lost much of their U during the disturbance episode, while samples with very high present $^{206}Pb/^{204}Pb$ ratios gained U (see Fig. 11). U gain is found mostly in samples from the Shabanie MIne, adjacent to the Shabani ultramafic complex which is intrusive into the gneisses, and it is particularly associated with alteration assemblages which include carbonate (RH*73*/*226*C, *227*A–E and *228*A, B, D; Moorbath et al., 1977).

Further efforts to correlate petrography of rock samples with loss or addition of U have generally not met with success: Banded migmatites and massive gneisses can both show either gain or loss of U. However, the association of U gain with the development of carbonate during alteration of the Shabani gneisses prompts us to consider the hypothesis that U mobilization might be associated with fluids active during rock formation, or in a later metamorphic event, or even during deep weathering in the mid- or late Archean. The paleodepth of the various Shabani gneiss samples below the Archean unconformity overlain by the Manjeri Formation (Bickle et al., 1975) cannot be ascertained. There is a marked metamorphosed regolith just below this contact; although the overall trace-element geochemistry of the samples does not betray any weathering effect (B. Luais, pers. commun., 1991), the mobility of U in deeply circulating meteoric water during the Archean cannot be excluded.

Any viable hypothesis involving fluid phase transport must account for occasional "selective" resetting of U–Pb and Rb–Sr clocks. Fluid phase composition might strongly influence the response of the Rb–Sr and U–Pb systems.

The gneisses in this study are mainly orthogneisses of the tonalite–trondhjemite–granodiorite (TTG) suite. During metamorphism up to medium grade no liberation of aqueous fluid would be expected in such rocks. In the transition from medium-grade to high-grade metamorphism, with the onset of partial melting and migmatitic segregation, water removed from minerals in dehydration reactions would become dissolved in a melt phase. Fluids may be liberated when partial melts crystallize, but the likely mobility of such fluids is not known. Interestingly, the fluid evolved upon crystallization of migmatite leucosomes often appears to be rich in CO_2 rather than H_2O (Touret and Olsen, 1985). The presence of CO_2 in a fluid greatly enhances the solubility of hexavalent U as $UO_2(CO_3)_2^{2-}$ or $UO_2(CO_3)_3^{4-}$ complexes (Langmuir, 1978; Michard et al., 1987; Villemont and Flehoc, 1989), while Rb and Sr are not particularly soluble in a CO_2-rich fluid phase. It is thus conceivable that during medium- to high-grade metamorphism of such felsic rocks the U–Pb system is disturbed, while the Rb–Sr system remains intact.

Under other circumstances an aqueous fluid might be generated, for example, due to prograde metamorphism of adjacent hydrothermally altered mafic volcanics, and this could account for mobilization of Rb and thus disturbance of the Rb–Sr system, while U might remain immobile, especially in a reducing environment. Thus, in the late Archean of Canada, Kerrich et al. (1987) have reported cases of Rb–Sr whole-rock dates appreciably younger than the real age of the rocks, and this they ascribe to the effects of long lasting hydrothermal activity.

Fig. 13 gives clear evidence that early decoupling of Th and U is a common feature of Archean basement TTG suites. In the $^{207}Pb/^{204}Pb$ bs. $^{206}Pb/^{204}Pb$ diagram, data for individual gneiss units plot in well-defined linear arrays, whereas in the $^{208}Pb/^{204}Pb$ vs. $^{206}Pb/^{204}Pb$ diagram the corresponding data generally scatter widely — good linear arrays for gneiss units in this plot are a rarity. From Fig. 13 it would also appear that U depletion is a more common phenomenon than U enrichment.

The significance of linear arrays in $^{207}Pb/^{204}Pb$ vs. $^{206}Pb/^{204}Pb$ diagrams (i.e. are they truly isochrons?) always has to be assessed with considerable caution. This is especially so in the case of rock units which show clear evi-

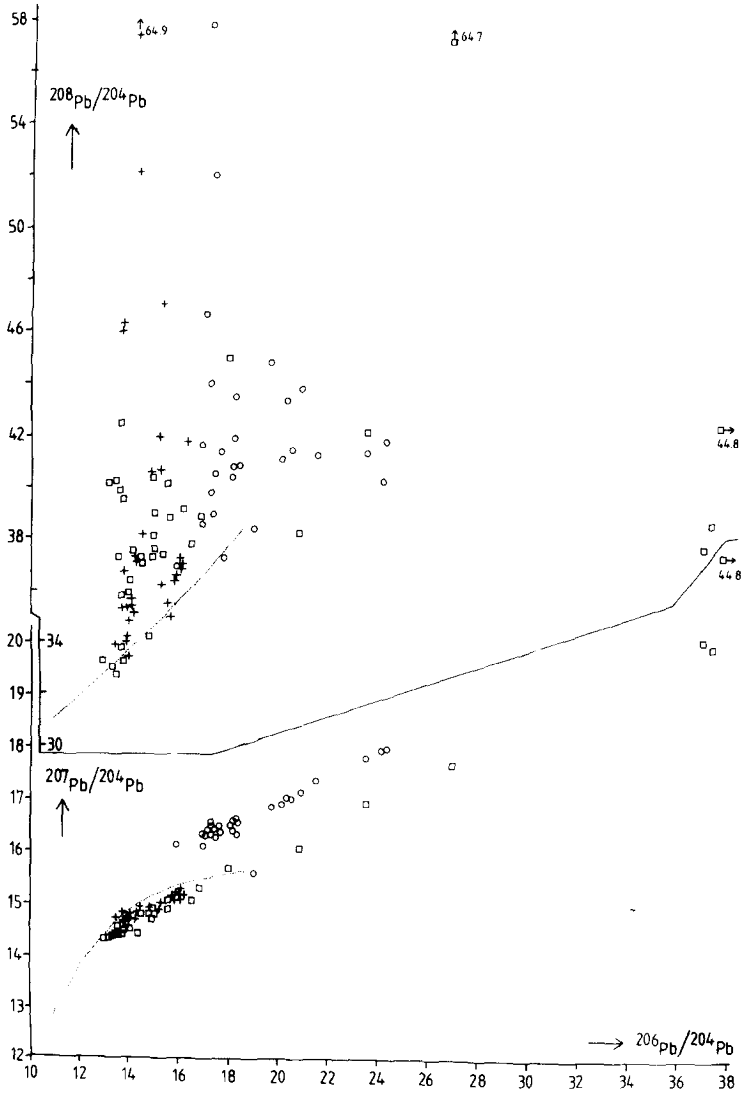

Fig. 13. $^{208}Pb/^{204}Pb$ and $^{207}Pb/^{204}Pb$ vs. $^{206}Pb/^{204}Pb$ plots of various Archean terrains: + = Lewisian (Moorbath et al., 1979); □ = Vredefort basement, South Africa (Hart et al., 1981); ○ = Sand River Gneisses, South Africa (Barton et al., 1983). Growth curves (as for Fig. 2) drawn in purely for reference.

dence of hydrothermal alteration, metamorphism or pervasive deformation which may have occurred markedly later than the original rock formation. However, the U–Pb system may also be disturbed in rocks which show no such petrographic evidence. In such cases post-magmatic U mobilization may only be evident from the corresponding $^{208}Pb/^{204}Pb$ vs. $^{206}Pb/^{204}Pb$ diagram, which therefore provides an important means to appraise the validity of Pb/Pb whole-rock isochron dates.

Several examples of spuriously old apparent Pb/Pb "isochron" ages have been reported, and these are generally the result of U depletion episodes long after the igneous protoliths were formed (Taylor, 1975; Griffin et al., 1978; Moorbath and Taylor, 1981, 1985; Welke and Nicolaysen, 1981; Moorbath et al., 1986). The Shabani gneisses studied in this paper provide an example of a Pb/Pb age which is clearly too young. However, it is the thesis of this paper that the combined application of the Rb–Sr and

Pb/Pb whole-rock isochron methods, together with Sm–Nd t_{DM} model ages and time-integrated Th/U ratios derived from $^{208}Pb/^{204}Pb$ vs. $^{206}Pb/^{204}Pb$ data, provides an adequate basis for resolving many of the problematical age discordances which are commonly found in the Archean gneiss terrains. In addition, the above discussion on the possible role of fluid phase composition in selective element mobility suggests that fluid inclusion studies combined with the isotopic methods might provide useful further insights into the early history of Archean cratons.

Acknowledgements

Critical comments from Tom Blenkinsop are greatly appreciated. Isotope work at Oxford University is supported by the Natural Environment Research Council. Grants for sampling trips were received from the Royal Society and the Research Board of the University of Zimbabwe.

References

Arden, J. and Gale, N.H., 1974. New electrochemical technique for separation of lead at trace levels from natural silicates. Anal. Chem., 46: 2–9.

Baldock, J.W. and Evans, J.A., 1988. Constraints on the age of the Bulawayan Group Metavolcanic Sequence, Harare Greenstone Belt, Zimbabwe. J. Afr. Earth Sci., 7: 795–804.

Barton, Jr., J.M., Ryan, B. and Fripp, R.E.P., 1983. Rb–Sr and U–Th–Pb studies of the Sand River Gneisses, central zone, Limpopo mobile belt. Spec. Publ. Geol. Soc. S. Afr., 8: 9–18.

Bickle, M.J., Martin, A. and Nisbet, E.G., 1975. Basaltic and peridotitic komatiites, stromatolites and a basal unconformity in the Belingwe greenstone belt, Rhodesia. Earth Planet. Sci. Lett., 27: 155–162.

Chauvel, C., Dupré, B., Todt, W., Arndt, N.T. and Hofmann, A.W., 1983. Pb and Nd isotopic correlation in Archean and Proterozoic greenstone belts. Eos (Trans. Am. Geophys. Union), 64: 330 (abstract).

DePaolo, D.J., 1981. Neodymium isotopes in the Colorado Front Range and Crust–Mantle evolution in the Proterozoic. Nature (London), 291: 193–196.

Dodson, M.H., Compston, W., Williams, I.S. and Wilson, J.F., 1988. A search for ancient detrital zircons in Zimbabwean sediments. J. Geol. Soc. London, 145: 977–983.

Fabiani, W., 1989. The geology of the Athens gold mine. D. Phil. Thesis, University of Zimbabwe, Harare (unpublished).

Griffin, W.L., Taylor, P.N., Hakkinen, J.W., Heier, K.S., Iden, I.K., Krogh, E.J., Malm, O., Olsen, K.I., Ormaasen, D.E. and Tveten, E., 1978. Archaean and Proterozoic crustal evolution in Lofoten–Vesteraelen, N. Norway. J. Geol. Soc. London, 135: 629–647.

Hamilton, P.J., 1977. Sr. isotope and trace element studies on the Great Dyke and Bushveld Mafic Phase and their relation to early Proterozoic magma genesis in Southern Africa. J. Petrol., 18: 24–52.

Hamilton, P.J., O'Nions, R.K. and Evensen, N.M., 1977. Sm–Nd dating of Archaean basic and ultrabasic volcanics. Earth Planet. Sci. Lett., 36: 263–268.

Hart, R.J., Welke, H.J. and Nicolaysen, L.O., 1981. Geochronology of the deep profile through Archaean basement at Vredefort, with implications for early crustal evolution. J. Geophys. Res., 86, B11: 10663–10680.

Hawkesworth, C.J., Moorbath, S., O'Nions, R.K. and Wilson, J.F., 1975. Age relationships between greenstone belts and "granites" in the Rhodesian Archaean craton. Earth Planet. Sci. Lett., 25: 251–262.

Hawkesworth, C.J., Bickle, M.J., Gledhill, A.R., Wilson, J.F. and Orpen, J.L., 1979. A 2.9 b.y. event in the Rhodesian Archaean. Earth Planet. Sci. Lett., 43: 285–297.

Hickman, M.H., 1974a. 3500-Myr-old granite in Southern Africa. Nature (London), 251: 295–296.

Hickman, M.H., 1974b. Geochronological study of the Rhodesian Craton and the Limpopo belt. Res. Inst. of Afr. Geol., Univ. of Leeds, Leeds, Annu. Rep. No. 18, pp. 61–62.

Hickman, M.H., 1978. Isotopic evidence for crustal reworking in the Rhodesian Archaean craton, Southern Africa. Geology, 6: 214–216.

Jahn, B.M. and Condie, K.C., 1976. On the age of Rhodesian greenstone belts. Contrib. Mineral. Petrol., 57: 317–330.

Kerrich, R., Fryer, B.J., King, R.W., Wilmore, L.M. and Van Hees, E., 1987. Crustal outgassing and LILE enrichment in major lithosphere structures, Archean Abitibi greenstone belt: Evidence on the source reservoir from strontium and carbon isotope tracers. Contrib. Mineral. Petrol., 97: 156–168.

Langmuir, D., 1978. Uranium–solution–mineral equilibria at low temperatures with application to sedimentary ore deposits. Geochim. Cosmochim. Acta, 42: 547–569.

MacGregor, A.M., 1951. Some milestones in the Precambrian of Southern Rhodesia. Proc. Geol. Soc. S. Afr., 54: 27–71.

Martin, A., 1978. The geology of the Belingwe–Shabani schist belt. Rhodesian Geol. Surv. Bull., No. 83, 220 pp.

Michard, A., Beaucare, C. and Michard, G., 1987. Uranium and rare earth elements in CO_2-rich waters from Vals des Bains (France). Geochim. Cosmochim. Acta, 51: 901–909.

Moorbath, S. and Taylor, P.N., 1981. Isotopic evidence for continental growth in the Precambrian. In: A. Kröner (Editor), Precambrian Plate Tectonics. Elsevier, Amsterdam, pp. 491–525.

Moorbath, S. and Taylor, P.N., 1985. Precambrian geochronology and the geological record. In: N.J. Snelling (Editor), The Chronology of the Geological Record. Mem. Geol. Soc. London, 10: 10–28.

Moorbath, S., Welke, H. and Gale, N.H., 1969. The significance of lead isotope studies in ancient, high grade metamorphic basement complexes, as exemplified by the Lewisian rocks of northwest Scotland. Earth Planet. Sci. Lett., 6: 245–256.

Moorbath, S., Wilson, J.F. and Cotterill, P., 1976. Early Archaean age for the Sebakwean Group at Selukwe, Rhodesia. Nature (London), 264: 536–538.

Moorbath, S., Wilson, J.F., Goodwin, R. and Humm, M., 1977. Further Rb–Sr age and isotope data on early and late Archaean rocks from the Rhodesian craton. Precambrian Res., 5: 229–239.

Moorbath, S., Taylor, P.N. and Jones, N.W., 1986. Dating the oldest terrestrial rocks: Fact and fiction. Chem. Geol., 57: 63–86.

Moorbath, S., Taylor, P.N., Orpen, J.L., Treloar, P.J. and Wilson, J.F., 1987. First direct radiometric dating of Archaean stromatolithic limestone. Nature (London), 326: 865–867.

Robertson, I.D.M., 1976. The geology of the country around Battlefields, Gatooma District. Rhodesia Geol. Surv. Bull., No. 76, 258 pp.

Stacey, J.S. and Kramers, J.D., 1975. Approximation of terrestrial lead isotope evolution by a two-stage model. Earth Planet. Sci. Lett., 26: 207–221.

Stowe, C.W., 1968. The geology of the country south and west of Selukwe. Rhodesia Geol. Surv. Bull., No. 59, 209 pp.

Stowe, C.W., 1979. A sequence of plutons in the Rhodesdale granite–gneiss terrane, Rhodesia. Trans. Geol. Soc. S. Afr., 82: 277–285.

Taylor, P.N., 1975. An early Precambrian age for migmatitic gneisses from Vika i Bø, Vesterålen, north Norway. Earth Planet. Sci. Lett., 27: 35–42.

Taylor, P.N., Jones, N.W. and Moorbath, S., 1984. Isotopic assessment of relative contributions from crust and mantle sources to the magma genesis of Precambrian granitoid rocks. Philos. Trans. R. Soc. London, Ser. A, 310: 605–625.

Touret, J. and Olsen, Sakiko N., 1985. Fluid inclusions in migmatites. In: J.R. Ashworth (Editor), Migmatites. Blackie, London, pp. 265–288.

Villemont, B. and Flehoc, C., 1989. U–Th fractionation by fluids in K-rich magma genesis in the Vico volcano, Central Italy. Earth Planet. Sci. Lett., 91: 312–326.

Welke, H.J. and Nicolaysen, L.O., 1981. A new interpretation procedure for whole-rock U–Pb systems applied to the Vredefort crustal profile. J. Geophys. Res., Gr 86, B11: 10681–10687.

Wilson, J.F., 1968. The geology of the country around Mashaba. Rhodesia Geol. Surv. Bull No. 62, 239 pp.

Wilson, J.F., 1979. A preliminary reappraisal of the Rhodesian Basement Complex. Spec. Publ. Geol. Soc. S. Afr., 5: 1–23.

York, D., 1969. Least squares fitting on a straight line, with correlated errors. Earth Planet. Sci. Lett., 5: 320–324.